Quantum Electronics **35** (11) 1015 – 1018 (2005)

PACS numbers: 42.62. –b; 52.38. –r; 43.28Mw
DOI: 10.1070/QE2005v035n11ABEH010355

Doppler effect for an optical discharge source of shock waves

V.N. Tishchenko

***Abstract*. The Doppler effect for a moving pulsating optical discharge producing periodic shock waves is considered. The manifestations of the effect are limited by the wave merging mechanism. The validity conditions were found for the effect in the case of a pulsating source of shock waves.**

Keywords: *optical pulsating discharge, merging mechanism of shock waves, Doppler effect.*

1. Introduction

This work continues the investigation of a quasi-continuous 'resonance' interaction of a pulsating optical discharge (POD) with a gas, which is based on POD properties and shock-wave merging mechanism (SWMM) [1, 2]. The POD is produced by repetitively pulsed laser radiation in the moving beam focus. For a certain combination of radiation and medium parameters ('resonance', the SWMM is engaged) the shock waves generated by the POD sparks merge together to form a long high-pressure quasi-stationary wave [1, 2]. The use of high-power lasers with a pulse repetition rate of ~ 100 kHz [3, 4] opens up the possibility of employing the POD and the SWMM in aerospace applications [2, 5 – 9].

The urgency of studying the Doppler effect (the effect in the subsequent discussion) stems from the fact that the POD is a unique sound source [10]: it is inherently point-like, the plasma-generated shock waves possess a power density of 10 – 20 kW cm^{-3}, the conversion efficiency amounts to ~ 30 %; the action of the SWMM limits the effect manifestation (see below). The difference of the POD from sound sources is as follows. The trains of repetitively pulsed laser radiation produce a wave field in which the ratio between the power in the low-frequency component and the total field power $\delta \sim f$ (f is the pulse repetition rate in the trains which follow with a frequency F, with $F \ll f$). For a high frequency f, the value $\delta \sim 1$. In acoustic sources, the quantity $\delta \sim F/f$, and therefore $\delta \ll 1$ %. The POD will enable solving the problem of point infrasound sources with a high conversion efficiency. Bunkin et al. noted that infrasound can emerge in the interaction of laser pulse trains with a liquid, the underlying method is density modulation whereby $\delta \sim F/f$. The conditions for the manifestation of SWMM were lacking in the experiments of Ref. [11].

The effect consists in the difference between the frequency f emitted by the source sound and the frequency f_g recorded by a receiver. When the source approaches an immobile receiver with a velocity V_0, the Doppler formula has the form [12]

$$f_g = \frac{f}{1 - M_0}, \tag{1}$$

where $M_0 = V_0/C_0$; C_0 is the sound velocity in a gas; the receiver is located on the z-line along which the source is moving.

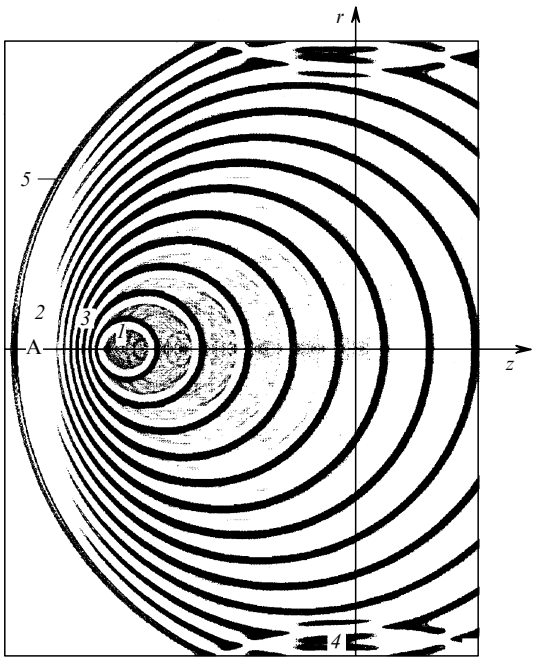

Figure 1. Fragment of the shock wave field for the instant $t = 1.04$ ms. The field as a whole has the shape of a sphere whose surface corresponds to the shock wave *5* generated by the first spark. The POD travels leftwards along the z axis from the intersection point of the axes z and r. The elevated pressure in the compression phase is shown in black [A – the 'sensor' position; *1* – POD; *2* – far-field zone (the pressure pulsations are weak); *3* – near-field zone; *4* – shock waves reflected from the wall].

V.N. Tishchenko Institute of Laser Physics, Siberian Branch, Russian Academy of Sciences, prosp. akad. Lavrent'eva 13/3, 630090 Novosibirsk, Russia; e-mail: tishenko@mail.nsk.ru

Received 14 June 2005; revision received 18 July 2005
Kvantovaya Elektronika **35** (11) 1015 – 1018 (2005)
Translated by E.N. Ragozin

The difference of a POD from an acoustic source is related to the SWMM action: at a distance from the POD ranging between 0 and $10R_d$ [1, 2] there occurs a structural change of the emitted signal. (Here, $R_d = (q/P_0)^{1/3}$ is the dynamic radius (m); q is the spark energy (J); and P_0 is the gas pressure (Pa).) In the limiting case, a quasi-stationary wave forms and the receiver measures the signal which rises with time.

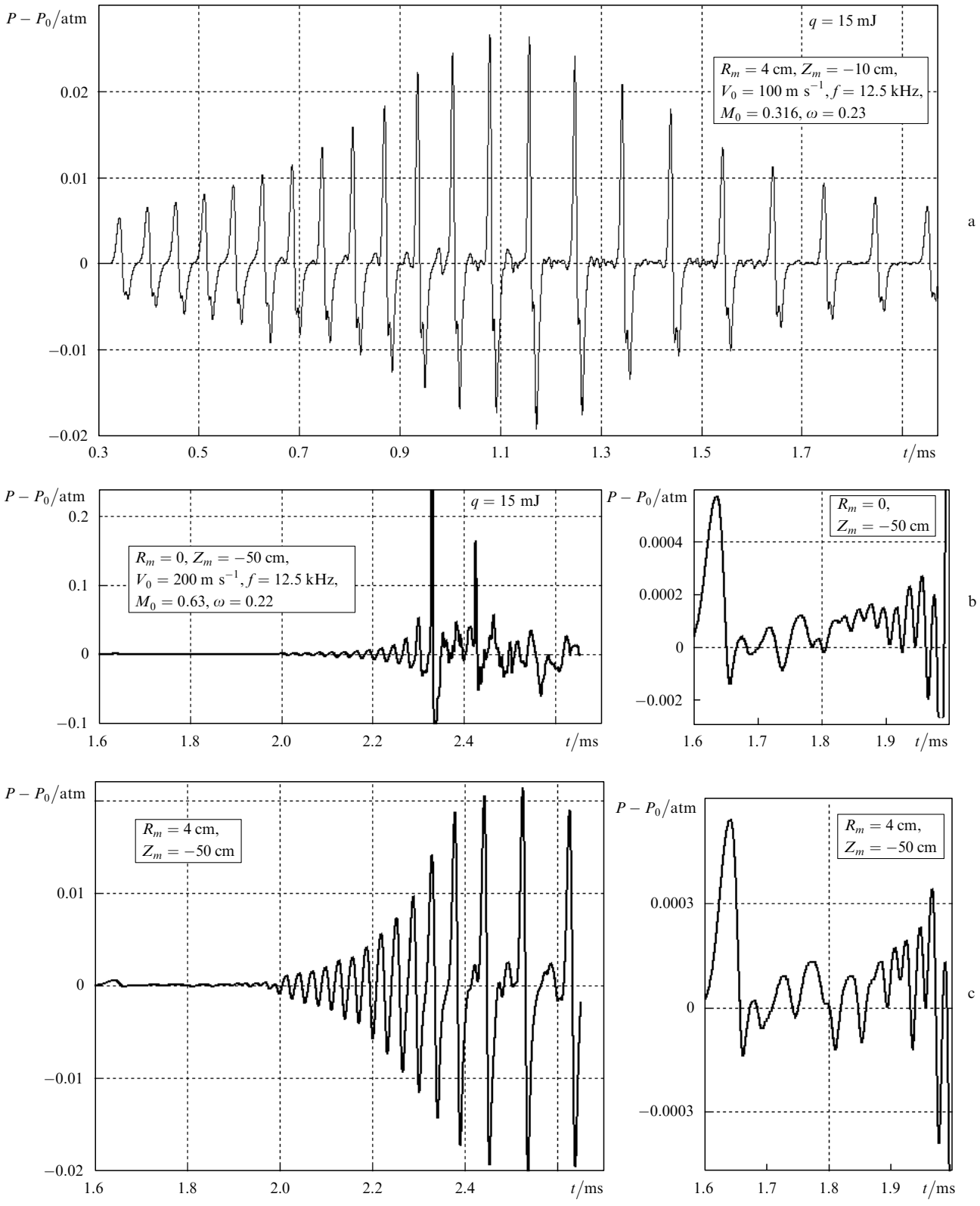

Figure 2. Time variation of the gas pressure at the points with coordinates R_m and Z_m. Parameters employed in the calculation: a POD with a repetition rate $f = 12.5$ kHz and an energy $q = 15$ mJ travels through argon ($P_0 = 1$ atm) with a velocity $V_0 = 100$ (a) and 200 m s^{-1} (b, c) from the point $Z = 0$ leftwards.

The POD generates periodic shock waves whose initial velocity V is much higher than C_0 and at a distance $\sim R_d$ the value of V becomes equal to C_0. When the distance between the observation point Z_m and the POD location Z_j is large, it can be assumed that the shock waves possess the velocity C_0. The frequency f_g begins to exhibit an appreciable dependence on V when the POD approaches the receiver by a distance $Z_m - Z_j < 3R_d$. The effect is determined in the measurement of a large number of waves. For the POD this implies that $Z_m - Z_j \gg R_d$.

For the effect to manifest itself the frequency f_g at which the shock waves arrive at the receiver should satisfy condition (1), which is valid in some region of the parameters f, q, V_0, C_0, P_0 (below, the D region).

The objective of our work was to determine the D region. Its boundaries were found from the SWMM criteria [1, 2] and verified by calculations in the two-dimensional axially symmetric approximation. The sparks were defined in the form of spherical regions of energy absorption in a time of ~ 0.2 μs. At the instant $t = 0$, the POD starts from a point $Z = 0$ and travels with a velocity V_0 towards the 'receiver' located at a point $Z_m/R_d \approx 100$. Figure 1 shows the calculated field of the shock waves when the POD parameters correspond to the boundary of the D region. By comparing the calculated data with formula (1), we assumed that f is the POD pulsation frequency and f_g is the frequency at which the shock waves arrive at the observation point; the value of f_g was obtained from calculations.

Figure 2 shows the temporal gas pressure distribution at points with the coordinates Z_m, R_m (R_m is the distance of the observation point from the z axis). For a low POD velocity and $R_m = 0$, the frequency f_g corresponds to the frequency obtained from (1). When $R_m > 0$ (Figs 2a and 2c), the geometrical factor begins to manifest itself as the POD approaches the receiver. For $t > 1$ ms, the POD moves away from the receiver and f_g lowers. Figures 2b and 2c depict the signals distorted by the action of the SWMM. One can see from Fig. 1 and Figs 2b and 2c, in front of the moving POD there forms a region consisting of two zones. Adjacent to the POD is a near-field zone in which the pressure exhibits regular pulsations. At a short distance from the observation point it is necessary to take into account the dependence of f_g on the shock velocity. The pressure pulsation frequencies in the far-field zone do not correspond to the effect, its length increases with time.

Figure 3 shows the region of effect manifestation found from the SWMM criteria. Here, $\omega = fR_d/C_0$ is the reduced POD pulsation frequency. Formula (1) can be expressed in terms of ω and M_0:

$$\omega_g = \frac{\omega}{1 - M_0}. \tag{2}$$

The region D in which ω_g satisfies relation (2) is bounded by the condition $\omega_0 > \omega < \omega_1$, where

$$\omega_0 \approx 2.5M_0, \tag{3}$$

$$\omega_1 \approx 0.65(1 - M_0). \tag{4}$$

The curves intersect at a point with the coordinates $\omega_{crit} = 0.52$, $M_{0crit} = 0.206$. For $\omega > \omega_0$, the POD produces shock waves in an unstable manner [2], the effect observation is hampered. For $\omega > \omega_1$, the difference in shape between the POD-produced shock waves (Figs 2b and 2c) and the measured signal arises from the SWMM action, which increases in importance as the ω_2 curve is approached. For $\omega > \omega_2 = 5.88(1 - M_0)^{1.5}$, the POD generates a quasi-stationary wave. We substitute formula (4) in relation (2) to find the limiting detector-sensed frequency $\omega_{g1} \sim 0.65$ that satisfies relation (2).

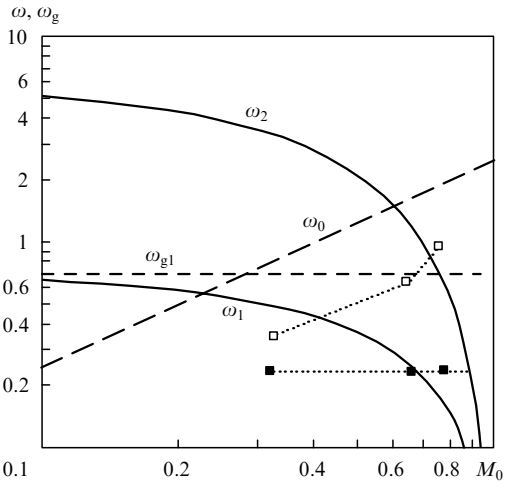

Figure 3. Boundary POD pulsation frequencies ω and receiver-sensed frequency ω_g versus velocity M_0 of POD travel. For $\omega < \omega_0$, the POD stably generates shock waves. Below the curve ω_1, the shock waves do not interact with each other, above ω_2 they produce a quasi-stationary wave. Full squares – POD parameters (ω, M_0) in the calculation, empty squares – frequencies ω_g perceived by the sensor. The squares with the parameters $M_0 = 0.316$ and 0.63 relate to the calculations represented in Figs 1a, 2b, and 2c; the limiting frequency ω_{gl} perceived by the sensor corresponds to the radiated frequency ω_1.

The validity of expressions (3) and (4) was confirmed by calculations. In particular, full squares with the coordinates $\omega = 0.22$ and $M_0 = 0.316$, 0.63, and 0.8 correspond to a series of calculations for which the pressure is shown in Fig. 2. The squares $\omega = 0.22$ and $M_0 = 0.316$ are situated in the D region, which is confirmed by calculation (see Fig. 2a). The points $\omega = 0.22$, $M_0 = 0.62$ and 0.8 are at the boundary or outside of the D region, which is evident from Figs 1 and 2b. In Fig. 3, to the full squares there correspond empty squares, which correspond to the values of ω_g calculated by formula (2). The empty square $\omega_g = 0.32$, $M_0 = 0.316$ is located below ω_{g1}, the limiting perceptible frequency. It determines the true value of the frequency ω_g perceived by the sensor. The empty squares lying above ω_{g1} may not be employed to denote the frequency ω_g. They serve to illustrate the existence of the limiting value $\omega_g = \omega_{g1} \sim 0.65$.

Let us make an estimate. For definiteness we assume the following parameters: the air, $P_0 \approx 10^5$ Pa, $C_0 = 340$ m s^{-1}, $V_0 = 100$ m s^{-1} ($M_0 = 0.294$), $q = 100$ J. We seek for the highest pulse-repetition rate f_1 beginning with which the effect does not manifest itself. Since $M_0 > M_{0crit}$, the frequency ω is limited by the value ω_1. From formula (4) we find $f_1 = 0.65(C_0 - V_0)(P_0/q)^{1/3} = 1560$ Hz.

The frequency ω_g obeys relation (2) when the POD possesses parameters lying in the D region and is remote from the receiver. However, for $(Z_m - Z_j)/R_d < Z_b \sim 3$ the frequency ω_g depends on the shock velocity and not on C_0. We determine the number of sparks and shock waves which the POD will produce in a length Z_b. Formulas (3) and (4) are represented in the form

$$Z_s > Z_{s0} \approx 0.4 \quad \text{for} \quad 0 < M_0 < M_{0\text{crit}}, \tag{5}$$

$$Z_s > Z_{s1} = \frac{1.5M_0}{1 - M_0} \quad \text{for} \quad M_{0\text{crit}} \leqslant M_0 < 1. \tag{6}$$

Here, $Z_s = (Z_j - Z_{j-1})/R_\text{d}$ is the interspark distance. To the D region there corresponds the inequality $Z_{s0} < Z_s > Z_{s1}$. Expressions (3), (4) and (5), (6) are different forms of writing the criteria for the manifestation of the Doppler effect. The number of sparks and shock waves is $N_v \approx Z_\text{b}/Z_s$. Putting $Z_s = Z_{s0}$ and $Z_s = Z_{s1}$, we obtain $N_{v0} = Z_\text{b}/Z_{s0} \approx 6$ for $0 < M_0 < M_{0\text{crit}}$ and $N_{v1} = Z_\text{b}/Z_{s1} \approx 2(1/M_0 - 1)$ for $M_{0\text{crit}} \leqslant M_0$. For $M_0 = 0.5$, the value $N_{v1} = 2$.

Therefore, the shock-wave merging mechanism limits the POD parameter region in which it is possible to observe the Doppler effect. The effect manifestation criteria are applicable to different gases and POD parameters, whose values (C_0 and P_0, V_0, f, and q) are taken into account in expressions for ω and M_0.

Acknowledgements. This work was supported by the Russian Foundation for Basic Research (Grant No. 03-02-17716) and the Siberian Branch, Russian Academy of Sciences (Grant No. 152).

References

1. Tishchenko V.N. *Kvantovaya Elektron.*, **33** (9), 823 (2003) [*Quantum Electron.*, **33** (9), 823 (2003)].
2. Tishchenko V.N., Apollonov V.V., Grachev G.N., Gulidov A.I., Zapryagaev V.I., Men'shikov Ya.G., Smirnov A.L., Sobolev A.V. *Kvantovaya Elektron.*, **34** (10), 941 (2004) [*Quantum Electron.*, **34** (10), 941 (2004)].
3. Tret'yakov P.K., Grachev G.N., Ivanchenko A.I., Krainev V.L., Ponomarenko A.G., Tishchenko V.N. *Dokl. Ross. Akad. Nauk*, **336** (4), 466 (1994).
4. Apollonov V.V., Kiiko V.V., Kislov V.I., Suzdal'tsev A.G., Egorov A.B. *Kvantovaya Elektron.*, **33** (9), 753 (2003) [*Quantum Electron.*, **33** (9), 753 (2003)].
5. Myrabo L.N., Raizer Yu.P. *AIAA Paper № 94-2451* (1994).
6. Tret'yakov P.K., Garanin A.F., Grachev G.N., Krainev V.L., Ponomarenko A.G., Tishchenko V.N. *Dokl. Ross. Akad. Nauk*, **351** (3), 339 (1996).
7. Tishchenko V.N. *Opt. Atmosf. Okean.*, **11** (2-3), 228 (1998).
8. Apollonov V.V., Tishchenko V.N. *Kvantovaya Elektron.*, **34** (12), 1143 (2004) [*Quantum Electron.*, **34** (12), 1143 (2004)].
9. Tishchenko V.N., Gulidov A.I. *Pis'ma Zh. Tekh. Fiz.*, **26** (19), 77 (2000).
10. Tishchenko V.N., Grachev G.N., Zapryagaev V.I., Smirnov A.V., Sobolev A.V. *Kvantovaya Elektron.*, **32** (4), 329 (2002) [*Quantum Electron.*, **32** (4), 329 (2002)].
11. Bozhkov A.I., Bunkin F.V., Kolomenskii Al.A., Malyarovskii A.I., Mikhalevich V.G. *Tr. Fiz. Inst. Akad. Nauk SSSR*, **156**, 123 (1984).
12. Landau L.D., Lifshitz E.M. *Fluid Mechanics* (Oxford: Pergamon Press, 1987).